Available online at www.sciencedirect.com
ScienceDirect
C. R. Mecanique 336 (2008) 685–692
COMPTES RENDUS MECANIQUE
http://france.elsevier.com/direct/CRAS2B/

An approximate yield criterion for anisotropic porous media

Shyam M. Keralavarma, A. Amine Benzerga *

Department of Aerospace Engineering, Texas A&M University, College Station, TX 77843-3141, USA

Received 8 October 2007; accepted after revision 30 July 2008

Available online 29 August 2008

Presented by Jean-Baptiste Leblond

Abstract

We derive a new yield function for materials containing spheroidal voids embedded in a perfectly-plastic anisotropic Hill-type matrix. Using approximate limit-analysis and a restricted set of trial velocity fields, analytical yield loci are derived for a hollow, spheroidal volume element containing a confocal spheroidal void. Alternatively, the yield loci are determined through numerical limit-analysis, i.e., employing a larger set of velocity fields. The numerical results are quasi-exact for transversely isotropic materials under axisymmetric loading. We show that an enhanced description of admissible microscopic deformation fields results in a close agreement between analytical and numerical macroscopic yield loci. ***To cite this article: S.M. Keralavarma, A.A. Benzerga, C. R. Mecanique 336 (2008).***

Résumé

Critère de plasticité approché pour milieux poreux anisotropes. On développe un nouveau critère de plasticité pour matériaux anisotropes contenant des cavités ellipsoïdales dans une matrice parfaitement plastique de type Hill. Le critère homogenéisé est obtenu par analyse limite approchée d'un volume élémentaire creux de forme ellipsoïdale contenant une cavité ellipsoïdale confocale, en utilisant un nombre réduit de champs de vitesse. Par ailleurs, on détermine numériquement les surfaces de charges en utilisant un ensemble plus large de champs de vitesse. Les résultats numériques sont quasi-exacts dans le cas de matériaux isotropes transverses sous chargement axisymétrique. On montre que la prise en compte de nouveaux champs admissibles de déformation améliore considérablement l'accord entre formes analytique et numérique du critère de plasticité macroscopique. ***Pour citer cet article : S.M. Keralavarma, A.A. Benzerga, C. R. Mecanique 336 (2008).***

Keywords: Porous media; Ductile metals; Void growth; Damage; Non-spherical voids; Micromechanics; Homogenization

Mots-clés : Milieux poreux ; Métaux ductiles ; Croissance de cavité ; Endommagement ; Cavités non-sphériques ; Micromécanique ; Homogénéisation

* Corresponding author.
E-mail addresses: skeralavarma@tamu.edu (S.M. Keralavarma), benzerga@aero.tamu.edu (A.A. Benzerga).

1631-0721/$ – see front matter
doi:10.1016/j.crme.2008.07.008

1. Introduction

Gurson [1] developed a micromechanics-based yield function for isotropic ductile porous media. He considered a spherical representative volume element (RVE) made of a rigid, perfectly plastic and *isotropic* material containing a concentric spherical void. The matrix was taken to obey the Von Mises yield criterion. His derivation was later shown to be amenable to Hill–Mandel homogenization of the kinematic kind, combined with limit-analysis of the chosen RVE subject to arbitrary loading conditions; see e.g. [2,3]. A unique feature of Gurson's criterion is that it constitutes, for the chosen RVE, a rigorous upper bound, which also happens to lie very close to the exact criterion.

Under large plastic deformations, however, the basic structural unit, i.e. the RVE itself, evolves. This microstructure evolution is only partially accounted for in the Gurson model, through the change in relative volume. But microstructure changes also occur due to development of plastic anisotropy, e.g., grain elongation or texture development, as well as to void shape evolution. The former was considered by Benzerga and co-workers [4–6] and the latter by Gologanu and co-workers [7–10] and Garajeu et al. [11]. The development of improved anisotropic models that account for coupling between plastic anisotropy and void shape effects has received limited attention in the literature, despite the practical need for such models. Since any change in void attributes, namely relative volume and aspect ratio, is not independent of the surrounding plastically deforming matrix, it only seems natural to adopt the same micromechanics framework used in previous studies to quantify the combined effects of plastic anisotropy and void shape on the effective behavior of porous plastic solids. Thus, the aim of the present note is to develop a yield criterion for such behavior in closed form. A similar attempt has recently been made by Monchiet et al. [12,13] who used a more restricted set of trial velocity fields. In addition, here we develop a numerical method to determine upper-bound yield loci through limit-analysis and using a large number of velocity fields. The numerically determined yield loci are quasi-exact for transversely isotropic materials under axisymmetric loading, and thus serve as a reference to assess the validity of the new analytical criterion.

2. Problem definition and approach

A spheroidal RVE of volume Ω is considered, which is made of a rigid perfectly plastic *orthotropic* matrix. Let $(\mathbf{e}_1, \mathbf{e}_2, \mathbf{e}_3)$ be an orthonormal basis associated with the principal directions of matrix anisotropy. A spheroidal coordinate system associated with the orthonormal basis $(\mathbf{e}_\lambda, \mathbf{e}_\beta, \mathbf{e}_\phi)$ is used for the analysis, for convenience of expressing the boundary conditions. In a cylindrical frame $(\mathbf{e}_r, \mathbf{e}_\theta, \mathbf{e}_z)$, with $\mathbf{e}_z$ aligned with the void axis, the base vectors of the spheroidal coordinate system are expressed as

$$\mathbf{e}_\lambda = \{a \sin\beta\, \mathbf{e}_r + b \cos\beta\, \mathbf{e}_z\}/\sqrt{g_{\lambda\lambda}}, \qquad \mathbf{e}_\beta = \{b \cos\beta\, \mathbf{e}_r - a \sin\beta\, \mathbf{e}_z\}/\sqrt{g_{\lambda\lambda}}, \qquad \mathbf{e}_\phi = \mathbf{e}_\theta \tag{1}$$

$$g_{\lambda\lambda} \equiv a^2 \sin^2\beta + b^2 \cos^2\beta, \qquad \begin{cases} a = c\cosh\lambda,\ b = c\sinh\lambda & \text{(p)} \\ a = c\sinh\lambda,\ b = c\cosh\lambda & \text{(o)} \end{cases} \tag{2}$$

where (p) and (o) are shorthand notations for "prolate" and "oblate", respectively, and c denotes half the focal distance. The current confocal spheroid has a and b as the axial and transverse semi-axes, respectively, and $e = 1/\cosh\lambda$ as the eccentricity. The RVE contains a confocal spheroidal void occupying volume ω. By convention, and where appropriate, subscripts 1 and 2 will refer to variable values at the void and RVE boundaries, respectively. Thus, with the choice of coordinates above, void and external RVE boundaries correspond to constant values of λ, designated λ_1 and λ_2, respectively. Alternatively, the geometry is characterized by two parameters, namely the porosity $f \equiv \omega/\Omega = a_1 {b_1}^2/a_2 {b_2}^2$ and the void aspect ratio, a_1/b_1.

A kinematic approach of homogenization theory is used to arrive at the macroscopic constitutive relations, in an Eulerian setting. The macroscopic stress, $\boldsymbol{\Sigma}$, and rate of deformation, $\mathbf{D}$, are obtained as volume averages over the RVE of the microscopic stress, $\boldsymbol{\sigma}$, and rate of deformation, $\mathbf{d}$, respectively:

$$\boldsymbol{\Sigma} = \langle \boldsymbol{\sigma} \rangle_\Omega, \qquad \mathbf{D} = \langle \mathbf{d} \rangle_\Omega \tag{3}$$

Using the Hill–Mandel lemma [14,15] in conjunction with a limit-analysis theorem, which strictly applies to infinitesimal transformations [16], the macroscopic yield surface in stress space is admittedly defined by

$$\boldsymbol{\Sigma} = \frac{\partial \Pi}{\partial \mathbf{D}}(\mathbf{D}) \tag{4}$$

Here, $\Pi(\mathbf{D})$ is the macroscopic plastic dissipation defined as the infimum of the volume-average of the plastic dissipation $\pi(\mathbf{d})$, the infimum being calculated over all admissible microscopic deformation fields. Formally,

$$\Pi(\mathbf{D}) = \inf_{\mathbf{d}\in\mathcal{K}(\mathbf{D})} \langle \pi(\mathbf{d}) \rangle_{\Omega}$$
$$\mathcal{K}(\mathbf{D}) = \left\{ \mathbf{d} \mid \exists \mathbf{v}, \forall \mathbf{x} \in \Omega,\ d_{ij} = \frac{1}{2}(v_{i,j} + v_{j,i}) \text{ and } \forall \mathbf{x} \in \partial\Omega,\ \mathbf{v} = \mathbf{D}.\mathbf{x} \right\} \tag{5}$$

For a given deviator $\mathbf{d}$, the microscopic plastic dissipation is defined as

$$\pi(\mathbf{d}) = \sup_{\boldsymbol{\sigma}^* \in \mathcal{C}} \boldsymbol{\sigma}^* : \mathbf{d} \tag{6}$$

the supremum being taken over all microscopic stresses that fall within the microscopic convex $\mathcal{C}$ of elasticity (or rigidity more precisely).

A quadratic Hill-type yield criterion [17] is assumed for the matrix material as in [6]. Thus, to the neglect of elasticity and hardening

$$\pi(\mathbf{d}) = \begin{cases} \sigma_1 d_{\text{eq}} & \text{(in the matrix)} \\ 0 & \text{(in the voids)} \end{cases} \tag{7}$$

where σ_1 is the yield stress in any arbitrarily chosen principal direction of orthotropy, say $\mathbf{e}_1$, and d_{eq} is the Hill equivalent strain rate defined as

$$d_{\text{eq}} = \sqrt{\frac{2}{3}\mathbf{d} : \hat{\mathbf{h}} : \mathbf{d}} \tag{8}$$

where the fourth-order tensor $\hat{\mathbf{h}}$ is the formal inverse of Hill's anisotropy tensor, $\mathbf{h}$; i.e., $\hat{\mathbf{p}} : \mathbf{p} = \mathbf{p} : \hat{\mathbf{p}} = \mathbf{J}$ where $\mathbf{p}$ and $\hat{\mathbf{p}}$ are given by $\mathbf{J} : \mathbf{h} : \mathbf{J}$ and $\mathbf{J} : \hat{\mathbf{h}} : \mathbf{J}$ respectively and $\mathbf{J}$ is the deviatoric projector [6]. In general, d_{eq} is defined up to a multiplicative constant, which is set consistent with the choice of σ_1. In the frame of material orthotropy, $\hat{\mathbf{h}}$ may be represented by a diagonal 6×6 matrix, thanks to Voigt reduction, with the diagonal elements, designated $\hat{h}_i$, as the anisotropy factors.

The RVE is subjected to homogeneous deformation rate boundary conditions. The following working assumptions are made so as to reduce the problem to one that is tractable analytically. First, the macroscopic deformation field is taken to be axially symmetric about one of the principal orthotropy directions, say $\mathbf{e}_3$, and has the form: $\mathbf{D} = D_{11}(\mathbf{e}_1 \otimes \mathbf{e}_1 + \mathbf{e}_2 \otimes \mathbf{e}_2) + D_{33}\mathbf{e}_3 \otimes \mathbf{e}_3$. Next, the void in the current configuration is supposed to retain a spheroidal shape and its axis is assumed to be aligned with the axis of symmetry of the imposed deformation, $\mathbf{e}_3$. Under such circumstances, the set of microscopic velocity fields are approximately taken to be axisymmetric, thus allowing to use the fields introduced by Lee and Mear [18] as trial ones in computing an upper bound of $\Pi(\mathbf{D})$. These fields are incompressible and supposedly complete. They are given in terms of infinite double series of associated Legendre functions of the first and second kinds. Their expressions are provided in [9] along with the constraints imposed by boundary conditions $(5)_2$ expressed in spheroidal coordinates.

Although, in general, none of the Lee–Mear fields can be an exact solution for anisotropic matrices, their use in (5) *a priori* leads to a rigorous upper bound for the macroscopic yield criterion. Furthermore, in the important special case of transversely isotropic matrices aligned with the voids and subject to axisymmetric loadings, the true velocity field can indeed be represented as a linear combination of the Lee–Mear fields.

3. Approximate yield criterion

Eqs. (4)–(6) provide a variational definition of the macroscopic yield surface. For the RVE of interest, the plastic dissipation writes

$$\Pi(\mathbf{D}) = \inf_{\mathbf{d}\in\mathcal{K}(\mathbf{D})} \frac{\sigma_1}{\Omega} \int_{\lambda_1}^{\lambda_2} \int_0^{\pi} \int_0^{2\pi} d_{\text{eq}} b g_{\lambda\lambda} \sin\beta \, \mathrm{d}\varphi \, \mathrm{d}\beta \, \mathrm{d}\lambda \tag{9}$$

For a chosen subset of $\mathcal{K}(\mathbf{D})$, explicit calculation of $\Pi(\mathbf{D})$ involves computation of d_{eq}, which depends on both plastic anisotropy and the choice of trial velocity fields. The approach followed in Gurson's original work [1] and later works based on it [9,6] was to use two trial velocity fields: a non-homogeneous "expansion" field ($\mathbf{v}^A$, $\mathbf{d}^A$) responsible for void growth, and a field $\mathbf{v}^B$ that corresponds to a uniform deviatoric strain rate, i.e.,

$$\mathbf{v} = A\mathbf{v}^A + B\mathbf{v}^B, \qquad \mathbf{v}^B = -\frac{r}{2}\mathbf{e}_r + z\mathbf{e}_z \tag{10}$$

The homogeneous boundary conditions, $\mathbf{v} = \mathbf{D}.\mathbf{x}$ in $(5)_2$, lead to linear constraints on the coefficients A and B of the velocity fields. Thus, irrespective of the specific choice of $\mathbf{v}^A$, the two independent components D_{11} and D_{33} of the macroscopic deformation field completely fix the multiplicative factors A and B of the chosen trial fields, eliminating the need for explicit minimization in Eq. (9). For the expansion field $\mathbf{v}^A$, we choose a combination of the Lee–Mear fields corresponding to coefficients B_{00}, B_{20}, B_{21} and B_{22}, with $B_{00} = 1$ by convention; see [9]. While coefficients A and B are fixed by the boundary conditions, the remaining B_{2i} coefficients remain free and thus can be used to "optimize" the yield criterion. Using the above decomposition of $\mathbf{v}$ in Eq. (8), along with the incompressibility of $\mathbf{v}^A$, leads to

$$d_{\text{eq}}^2 = A^2 d_{\text{eq}}^{A2} + 2hAB d_{33}^A + hB^2, \qquad h \equiv (\hat{h}_1 + \hat{h}_2 + 4\hat{h}_3)/6 \tag{11}$$

with d_{eq}^A defined similar to d_{eq} in (8).

Subsequently, a parametric representation of the yield surface is formally obtained. Using Eq. (4), it can be shown that

$$\frac{\partial \Pi}{\partial A} = \frac{3c^3}{a_2 b_2^2}\Sigma_h, \qquad \frac{\partial \Pi}{\partial B} = \Sigma_{33} - \Sigma_{11}$$
$$\Sigma_h \equiv 2\alpha_2 \Sigma_{11} + (1 - 2\alpha_2)\Sigma_{33}, \qquad \alpha_2 \equiv \frac{D_{11}^A}{2D_{11}^A + D_{33}^A} \tag{12}$$

The definition of parameter α_2 involves the components of $\mathbf{D}$ through the expansion field $\mathbf{D}^A = \langle \mathbf{d}^A \rangle_\Omega$, and therefore depends on the unknown coefficients B_{2i} and associated Legendre functions [9]. Eq. (12) defines a representation of the yield locus in which the ratio A/B acts as the parameter. Explicit calculation of the plastic dissipation and elimination of the parameter from the above equations yield the closed form expression for the macroscopic yield function. However, the mathematical complexity involved in performing the above steps necessitates the introduction of approximations which, in some but not all instances, are similar to those used in [9]. First, d_{eq} in (9) is replaced with its root mean square value over the surface of the current spheroid $\mathcal{S}_\lambda$ confocal with the void. This approximation actually preserves the upper bound character of the approach. Using the change of variable $x = c^3/ab^2$, an upper bound on $\Pi(\mathbf{D})$ can be written as, keeping the same notation for convenience:

$$\Pi(\mathbf{D}) = \sigma_1 x_2 \int_{x_2}^{x_1} \langle d_{\text{eq}}^2 \rangle_{\mathcal{S}_\lambda}^{1/2} \frac{\mathrm{d}x}{x^2}, \qquad \langle d_{\text{eq}}^2 \rangle_{\mathcal{S}_\lambda} = A^2 P(x) + hB^2 + 2hAB\,Q(x) \tag{13}$$

where $P(x)$ and $Q(x)$ are single-valued functions; in anticipation of further approximations below, their expressions are omitted for brevity. Next, employing a unified notation with $u = x$ for prolate ($a_1 > b_1$) and $u = \frac{x}{x+1}$ for oblate ($a_1 < b_1$) cavities, the functions $P(x)$ and $Q(x)$ are replaced with $F(u)$ and $G(u)$, which are defined through $P(x) = F^2(u)u^2$ and $Q(x) = F(u)G(u)u^2$, so that Eq. (13) now reads

$$\Pi(\mathbf{D}) = \sigma_1 x_2 \int_{u_2}^{u_1} \sqrt{\left[AF(u) + hBG(u)\right]^2 u^2 + B^2 H^2(u)}\, \frac{\mathrm{d}u}{u^2}$$
$$H(u) \equiv \sqrt{h\left(1 - hG^2(u)u^2\right)} \tag{14}$$

In order to reduce the plastic dissipation integral to a Gurson-like form, functions $F(u)$, $G(u)$ and $H(u)$ are respectively replaced by constants $\bar{F}$, $\bar{G}$ and $\bar{H}$, to be specified. This can be further justified considering that, function $F(u)$ has a low range of variation in the domain of u, despite its complicated expression, and that $G(u)$ and $H(u)$, which

result from the "crossed" term contribution in $(11)_1$, have little effect on the yield criterion in the isotropic case [9]. Thus,

$$\Pi(\mathbf{D}) = \sigma_1 x_2 \int_{u_2}^{u_1} \sqrt{A'^2 u^2 + B'^2}\,\frac{\mathrm{d}u}{u^2}, \quad A' \equiv \bar{F}A + h\bar{G}B,\ B' \equiv \bar{H}B \tag{15}$$

Evaluation of the integral in (15), followed by elimination of the parameter A/B between Eqs. $(12)_1$ and $(12)_2$ lead to the yield criterion:

$$\frac{C}{\sigma_1^2}(\Sigma_{33} - \Sigma_{11} + \eta\Sigma_h)^2 + 2(g+1)(g+f)\cosh\kappa\frac{\Sigma_h}{\sigma_1} - (g+1)^2 - (g+f)^2 = 0 \tag{16}$$

where

$$C \equiv \frac{1}{\bar{H}^2}, \qquad \eta \equiv -3x_2\frac{h\bar{G}}{\bar{F}}, \qquad \kappa \equiv \frac{3}{\bar{F}}, \qquad g \equiv \begin{cases} 0 & \text{(p)} \\ x_2 & \text{(o)} \end{cases} \tag{17}$$

Note that the final form of the yield function is identical to that proposed in [9]. However, here the parameters κ, η and C not only depend upon the porosity and void aspect ratio but also on the anisotropy factors, $\hat{h}_i$.

Determining the criterion parameters amounts to specifying constants $\bar{F}$, $\bar{G}$ and $\bar{H}$, which depend on coefficients B_{2i} of the expansion velocity field. Here, we constrain these not to depend on material anisotropy. Parameter $\bar{F}$ is determined so as to ensure that the analytical yield locus is close to the actual one for purely hydrostatic loading. We require that use of $\bar{F}$ in place of $F(u)$ in (14) yield the actual value of the integral for the case of $B = 0$, i.e.,

$$\bar{F} = \left(\ln\frac{u_1}{u_2}\right)^{-1} \int_{u_2}^{u_1} F(u)\frac{\mathrm{d}u}{u} \tag{18}$$

For given u_1 and u_2, the best choice of $\bar{F}$ is obtained by minimizing the above integral with respect to coefficients B_{2i}, following arguments developed in [9]. This minimization is carried out numerically to guide further approximations aimed at obtaining closed form solutions. First, a variant of function $F(u)$, as obtained in [9], is minimized with respect to the B_{2i}'s, for fixed u and subject to the additional constraint that deformation be homogeneous on each surface $\mathcal{S}_\lambda$. This results in lengthy expressions $B_{2i}(u)$, which completely define the expansion field $\mathbf{v}^A$. These expressions are then used to determine parameter α_2 through $(12)_4$ leading to

$$\alpha_2 = \begin{cases} \dfrac{(1+e_2^2)}{(1+e_2^2)^2 + 2(1-e_2^2)} & \text{(p)} \\ \dfrac{(1-e_2^2)(1-2e_2^2)}{(1-2e_2^2)^2 + 2(1-e_2^2)} & \text{(o)} \end{cases} \tag{19}$$

Interestingly, in the prolate case, use of the so-determined $B_{2i}(u)$ expressions results in a function $F(u)$ that gives a close approximation of the true $F(u)$ that minimizes integral (18), irrespective of bounds u_1 and u_2 and for all values of the anisotropy factors $\hat{h}_i$ that were investigated. The expression thus obtained for $F(u)$ is yet too complicated and an approximate fit to this function is actually used in (18) to compute $\bar{F}$. The fit is more concise when expressed in terms of the eccentricity e instead of u:

$$\begin{aligned} F(e) &= \sqrt{\frac{9}{5}(4h + 8h_a - 7h_t)\frac{(1-e^4)}{(3+e^4)^2} + 3h_t} \\ h_t &\equiv \frac{\hat{h}_1 + \hat{h}_2 + 2\hat{h}_6}{4}, \qquad h_a \equiv \frac{\hat{h}_4 + \hat{h}_5}{2} \quad \text{(p)} \end{aligned} \tag{20}$$

In the oblate case, however, the same approach does not lead to satisfactory minimization of the integral in (18). Hence, a heuristic function $F(u)$ is used, similar to that proposed in [9], given by

$$F(u) = \sqrt{\frac{4}{5}(h + 2h_a + 2h_t)\left(1 + u + 2u^{5/2} - 3u^5\right)} \quad \text{(o)} \tag{21}$$

This function is found to give acceptable agreement with the (numerically determined) function that minimizes the integral in Eq. (18) with respect to the B_{2i}'s for all values of u_1, u_2 and $\hat{h}_i$ tested.

Therefore, parameter κ can be determined by substituting (20) or (21) into (18), in conjunction with $(17)_3$. For the prolate case, since the integral cannot be evaluated in closed form, the mean of $F^2(e)$ is evaluated using Eq. (18) and the square root of this value is assigned to $\bar{F}$. It is verified numerically that for all values of e_1 and e_2, the two values are close to each other. Thus,

$$\kappa = \begin{cases} \sqrt{3}\left\{\dfrac{1}{\ln f}\left[\dfrac{2}{3}\ln\dfrac{1-e_2^2}{1-e_1^2}+\dfrac{3+e_2^2}{3+e_2^4}-\dfrac{3+e_1^2}{3+e_1^4}+\dfrac{1}{\sqrt{3}}\left(\tan^{-1}\dfrac{e_2^2}{\sqrt{3}}-\tan^{-1}\dfrac{e_1^2}{\sqrt{3}}\right)\right.\right. \\ \qquad \left.\left.-\dfrac{1}{2}\ln\dfrac{3+e_2^4}{3+e_1^4}\right]\dfrac{4h+8h_a-7h_t}{10}+\dfrac{4(h+2h_a+2h_t)}{15}\right\}^{-1/2} & \text{(p)} \\ \dfrac{3}{2}\left(\dfrac{h+2h_a+2h_t}{5}\right)^{-1/2}\left\{1+\dfrac{1}{\ln\frac{g_f}{g_1}}\left\{(g_f-g_1)+\dfrac{4}{5}\left(g_f^{5/2}-g_1^{5/2}\right)-\dfrac{3}{5}\left(g_f^5-g_1^5\right)\right\}\right\}^{-1} & \text{(o)} \end{cases} \tag{22}$$

with $g_f \equiv g/(g+f)$ and $g_1 \equiv g/(g+1)$. In the case of spherical voids, (22) reduces to $\kappa = 3/2\sqrt{5/(h+2h_a+2h_t)}$ and in the limit of cylindrical voids $\kappa = \sqrt{3/h_t}$, which are results established in [6].

The remaining parameters C and η, which are connected to the constants $\bar{G}$ and $\bar{H}$, are determined by forcing the approximate yield locus to pass through and be tangent to known exact points on the two-field yield locus. Following derivations similar to those in [9], this leads to expressions for C and η given by

$$\begin{aligned} \eta &= -\frac{\kappa Q^*(g+1)(g+f)\,\mathrm{sh}}{(g+1)^2+(g+f)^2+(g+1)(g+f)[\kappa H^*\,\mathrm{sh}-2\,\mathrm{ch}]} \\ C &= -\frac{\kappa(g+1)(g+f)\,\mathrm{sh}}{(Q^*+\eta H^*)\eta}, \quad \mathrm{sh}\equiv\sinh(\kappa H^*),\ \mathrm{ch}\equiv\cosh(\kappa H^*) \end{aligned} \tag{23}$$

where H^* and Q^* are the values provided in [9] for Σ_h/σ_1 and $(\Sigma_{33}-\Sigma_{11})/\sigma_1$, respectively, multiplied by $\sqrt{h}$, where h is the anisotropy factor given by $(11)_2$.

It may be verified that in the case of an isotropic matrix, the proposed criterion (16) reduces to that of Gologanu et al. [9] for oblate voids. For prolate voids, the two criteria are different due to the distinct approaches followed in determining κ. The new isotropic criterion is an improved version of Gologanu et al.'s but the yield loci are very close to each other. For spherical and cylindrical voids in a transversely isotropic matrix the proposed criterion reduces to that of Benzerga and Besson [6]. For a general orthotropic matrix, the two criteria differ in the quadratic term of the yield function. For spherical and cylindrical voids in an isotropic matrix Gurson's criteria [1] are recovered.

4. Validation

In order to assess the validity of the approximations introduced in deriving the new analytical yield criterion, the latter is compared, for selected sets of the anisotropy factors, with a criterion determined numerically. To that end, a numerical method is developed to determine the yield loci for orthotropic materials containing spheroidal voids, similar to the one developed in [9] for the isotropic case. The method consists of minimizing the macroscopic plastic dissipation in (5) for axisymmetric radial loading paths, using a large number of velocity fields from the Lee–Mear expansion, i.e., larger than could be kept in our analytical derivation of the effective yield criterion. While the true deformation field is admittedly not axisymmetric in the general case of orthotropy, the upper-bound nature of the limit analysis approach ensures that the yield locus so derived lies external to the true yield surface. Moreover, in the special case of transverse isotropy and axisymmetric loading the numerical yield locus will be quasi-exact, i.e., exact up to errors due to a cutoff in the Lee–Mear fields. This is so because of the assumed completeness of the velocity fields and the fact that higher order terms in the expansion are fast decaying fields. All examples to follow focus on this special case of transverse isotropy.

The numerical yield loci are generated using seven velocity fields from the Lee–Mear expansion, corresponding to the field coefficients B_{00}, B_{2i}, $i = 0,\ldots,2$, and C_{2i}, $i = 0,\ldots,2$. Based on tests conducted, it is our observation that using a larger number of velocity fields (up to twenty) in the numerical calculations leads to negligible improvement

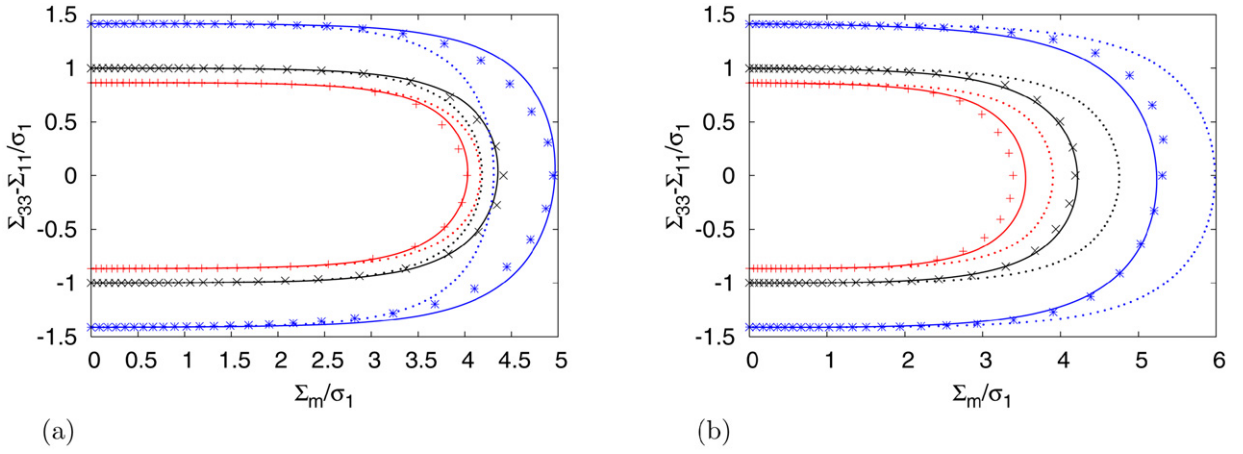

Fig. 1. Approximate yield loci (solid lines) and numerical yield loci (discrete points) for Al (+), Zr (∗) and isotropic matrix (×), using $f = 0.001$ and (a) prolate voids ($a_1/b_1 = 5$); (b) oblate voids ($a_1/b_1 = 1/5$). Dotted lines are for loci from [12].

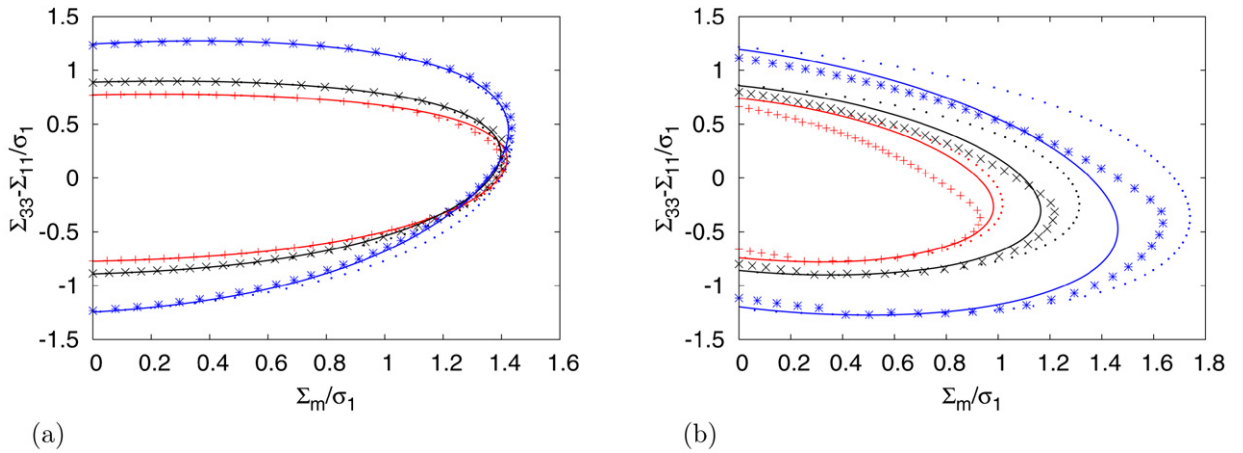

Fig. 2. Approximate yield loci (solid lines) and numerical yield loci (discrete points) for Al (+), Zr (∗) and isotropic matrix (×), using $f = 0.1$ and (a) prolate voids ($a_1/b_1 = 5$); (b) oblate voids ($a_1/b_1 = 1/5$). Dotted lines are for loci from [12].

in the upper-bound obtained. Two sets of transversely isotropic material properties are used based on tabulations in [5]: $\{\hat{h}_1 = \hat{h}_2 = \hat{h}_6 = 1.125, \hat{h}_3 = 0.5625, \hat{h}_4 = \hat{h}_5 = 0.2727\}$ and $\{\hat{h}_1 = \hat{h}_2 = \hat{h}_6 = 0.8571, \hat{h}_3 = 2.571, \hat{h}_4 = \hat{h}_5 = 2.000\}$. These sets are representative of Aluminum (Al) plates and Zircaloy (Zr) sheets, respectively. For comparison, calculations are also carried out for the isotropic case.

Fig. 1 summarizes the comparison between analytical and numerical yield loci for a low value of porosity $f = 0.001$ and two values of the void aspect ratio, a_1/b_1. The numerical yield loci are shown as discrete points. Each point corresponds to a numerical minimization performed for a fixed value of the stress ratio Σ_{33}/Σ_{11}. The plots show the macroscopic effective stress, $\Sigma_{33} - \Sigma_{11}$, plotted against the mean normal stress, Σ_m. Evidently, it is desirable that the approximate yield locus lies outside of the numerical one. While this is not always the case, the correspondence between the two is quite remarkable. Results corresponding to the criterion developed by Monchiet et al. [12] are also shown using dotted lines for comparison. Their criterion, which is a significant improvement of previous models, does not capture well the effect of material anisotropy in the prolate case (Fig. 1(a)) and is found to be too conservative in the oblate case (Fig. 1(b)).

Fig. 2 shows similar results for a much higher value of the porosity $f = 0.1$. The yield surfaces show a higher degree of distortion is this case. While the above observations generally apply, a discrepancy is noted for oblate voids near the hydrostatic axis between analytical and numerical loci. For applications to ductile fracture, this discrepancy

is a minor one, however, since (i) for structural materials, void coalescence occurs at values of f smaller than 0.1 [19]; and (ii) most practical loadings fall outside of the extreme stress triaxiality region.

5. Conclusion

The framework of homogenization was used to derive a yield criterion for anisotropic porous materials using an approximate limit-analysis. The new yield criterion combines the effects of spheroidal voids and matrix anisotropy in the form of Hill-type orthotropy. A semi-analytical approach was used to arrive at a closed form expression for the yield function. The new model was shown to yield close agreement with numerically derived, quasi-exact upper-bound yield loci for transversely isotropic materials. In the general case of orthotropy, the numerical results also represent an upper bound that could be used as an approximate yield locus. The new model thus constitutes an improvement of previously available models for anisotropic porous media, which have received little attention in the literature. Use of the new criterion in finite element simulations of ductile fracture requires, in addition, evolution laws for the microstructural variables, i.e., porosity and void aspect ratio. These need to be calibrated using finite element simulations on porous unit cells to obtain reliable estimates of the evolution of the microstructure with deformation. This work is in progress and results will be presented in future publications.

References

[1] A.L. Gurson, Continuum theory of ductile rupture by void nucleation and growth: Part I. Yield criteria and flow rules for porous ductile media, J. Eng. Mat. Tech. 99 (1977) 2–15.
[2] G. Perrin, Contribution à l'étude théorique de la rupture ductile des métaux, PhD thesis, École Polytechnique, 1992.
[3] J.B. Leblond, Mécanique de la rupture fragile et ductile, Hermes Science Publications, Lavoisier, 2003.
[4] A.A. Benzerga, J. Besson, A. Pineau, Modèle couplé comportement–endommagement ductile de tôles anisotropes, in: B. Peseux, et al. (Eds.), Actes du 3ème Colloque National en Calcul des Structures, Presses Académiques de l'Ouest, 1997, pp. 673–678.
[5] A.A. Benzerga, Rupture ductile des tôles anisotropes, PhD thesis, École Nationale Supérieure des Mines de Paris, 2000.
[6] A.A. Benzerga, J. Besson, Plastic potentials for anisotropic porous solids, Eur. J. Mech. 20 (3) (2001) 397–434.
[7] M. Gologanu, J.-B. Leblond, J. Devaux, Approximate models for ductile metals containing non-spherical voids – case of axisymmetric prolate ellipsoidal cavities, J. Mech. Phys. Solids 41 (11) (1993) 1723–1754.
[8] M. Gologanu, J.-B. Leblond, J. Devaux, Approximate models for ductile metals containing non-spherical voids – case of axisymmetric oblate ellipsoidal cavities, J. Eng. Mat. Tech. 116 (1994) 290–297.
[9] M. Gologanu, J.-B. Leblond, G. Perrin, J. Devaux, Recent extensions of Gurson's model for porous ductile metals, in: P. Suquet (Ed.), Continuum Micromechanics, in: CISM Lectures Series, Springer, New York, 1997, pp. 61–130.
[10] M. Gologanu, Étude de quelques problèmes de rupture ductile des métaux, PhD thesis, Université Paris 6, 1997.
[11] M. Garajeu, J.C. Michel, P. Suquet, A micromechanical approach of damage in viscoplastic materials by evolution in size, shape and distribution of voids, Comput. Methods Appl. Mech. Engrg. 183 (2000) 223–246.
[12] V. Monchiet, C. Gruescu, E. Charkaluk, D. Kondo, Approximate yield criteria for anisotropic metals with prolate or oblate voids, C. R. Mecanique 334 (2006) 431–439.
[13] V. Monchiet, O. Cazacu, E. Charkaluk, D. Kondo, Macroscopic yield criteria for plastic anisotropic materials containing spheroidal voids, Int. J. Plasticity 24 (2008) 1158–1189.
[14] J. Mandel, Contribution théorique à l'étude de l'écrouissage et des lois de l'écoulement plastique, in: 11th International Congress on Applied Mechanics, Springer, Berlin, 1964, pp. 502–509.
[15] R. Hill, The essential structure of constitutive laws for metal composites and polycrystals, J. Mech. Phys. Solids 15 (1967) 79–95.
[16] P. Suquet, Plasticité et homogénéisation, Thèse d'Etat, Université Pierre et Marie Curie, Paris VI, 1982.
[17] R. Hill, A theory of yielding and plastic flow of anisotropic solids, Proc. Roy. Soc. London A 193 (1948) 281–297.
[18] B.J. Lee, M.E. Mear, Axisymmetric deformation of power–law solids containing a dilute concentration of aligned spheroidal voids, J. Mech. Phys. Solids 40 (8) (1992) 1805–1836.
[19] A.A. Benzerga, J. Besson, A. Pineau, Anisotropic ductile fracture. Part I: Experiments, Acta Mater. 52 (2004) 4623–4638.